Journal of Molecular Spectroscopy 382 (2021) 111514

Contents lists available at ScienceDirect

Journal of Molecular Spectroscopy

journal homepage: www.elsevier.com/locate/yjmsp

On the formation and spectral signatures of magnesacyclopropene (c-MgC_2H_2)

Kimberley N. Poland [a], C. Zachary Palmer [a], Ava Chard [b], Steven R. Davis [a], Ryan C. Fortenberry [a,*]

[a] Department of Chemistry and Biochemistry, University of Mississippi, University, MS, United States
[b] Department of Chemistry and Biochemistry, Northern Arizona University, Flagstaff Arizona, United States

ARTICLE INFO

Keywords:
Astrochemistry
Organometallic chemistry
Coupled cluster theory
Vibrational spectroscopy
Rotational spectroscopy

ABSTRACT

Magnesium's divalent nature and likely importance as a building block for planet formation lends it credence to being a reasonable replacement for oxygen in organometallic species found in the interstellar medium (ISM). With the natural abundance of acetylene and magnesium and the presence of propylene oxide in the ISM, a natural next-step for astrochemical exploration of such organometallic molecules would be magnesacyclopropene (c-MgC_2H_2). The present work utilizes a combination of highly accurate quantum chemical quartic force field approaches to provide fundamental anharmonic frequencies to assist in the observation of the $1\ ^1A_1$ and $1\ ^3B_2$ electronic states of c-MgC_2H_2 and potential energy surface (PES) scans of Mg dissociation to assist in possible formation pathways of this molecule. The $1\ ^3B_2$ ω_7 mode is less than 0.5 cm^{-1} above previous theory implying that the current work is accurate and reliable. The $1\ ^3B_2$ electronic state is lower in energy than the $1\ ^1A_1$ by approximately 10.3 kcal/mol, while the $1\ ^1A_1$ electronic state is more rovibrationally observable with three fundamental vibrational frequencies having intensities of greater than 100 km/mol and a dipole moment of 5.47 D. The PES scan of the Mg dissociation shows a flatter well for the $1\ ^3B_2$, rather than the $1\ ^1A_1$, electronic state offering overlap between the vibronic levels. While radiative association is likely required for formation of c-MgC_2H_2, the triplet surface is rather flat reducing the energy gaps between vibrational levels. Additionally, the singlet surface in many ways mirrors the triplet providing for both likely and low-energy transitions between the states.

1. Introduction

Following the observation of molecular absorption spectra emitted by stars in the 1930s, the idea that the universe is primarily atomic with only a small amount of diatomic character has shifted to the realization that the universe is significantly molecular [1]. While hydrogen and helium comprise roughly 99% of the universe, the other notable atomic citizens of the universe include O, C, Ne, N [2], Mg [3], S [4], Si [5], and Fe [6], listed roughly in decreasing order of abundance [7]. Most notably, organic molecules such as benzonitrile [8] and C_2H_2 [9] have been detected with a few hundred others also now known [10]. Fewer inorganic and organometallic species have been observed thus far, though, but this has been shifting as additional reference data have been produced for such species [11] leading to new observations [12].

One such atom in the aforementioned list is magnesium. The twelfth element on the periodic table has been hypothesized to be a necessary building block for planet formation, evidenced by higher concentration values in planet-hosting stars and a deficit in those not hosting planets [13–17]. Additionally, molecules containing it have been known to exist towards various interstellar sources for more than 25 years now. These include MgNC, MgCN, MgCCH, MgC_3N, and MgC_4H [12,14,18,19] to date; all could be classified as organometallic. The relative abundance of Mg atoms and the rich astrochemistry of hydrocarbons makes the connection for molecules of this type to be worth exploring for astrochemical detection. As a result, this work will explore the chemistry and spectral features of magnesacyclopropene (c-MgC_2H_2), a combination of Mg atoms with the relatively abundant C_2H_2 hydrocarbon.

Magnesium is divalent much like oxygen. However, the lack of lone pairs and only two electrons in the valence shell produces bond angles in Mg-containing species in the realm of 180° [13], whereas oxygen is closer to 104.5°. The chiral propylene oxide molecule has been detected towards Sagittarius B2 [20] implying that epoxide chemistry is likely

* Corresponding author.
E-mail address: r410@olemiss.edu (R.C. Fortenberry).

https://doi.org/10.1016/j.jms.2021.111514
Received 8 June 2021; Received in revised form 16 July 2021; Accepted 6 August 2021
Available online 28 October 2021

occurring in at least this region of the ISM. Hence, magnesium replacement in the form of c-MgC_2H_2 as an initial exploration is possible opening new motifs for organometallic species.

Early theoretical work has explored the lowest singlet and triplet PES of [Mg, C_2, H_2] and its isomers using HF/6-31G* and MP2/3-21G* levels of theory. Therein, the linear, singlet state is determined to be the ground state [21]. Later density functional theory (DFT) calculations support the experimental observations in which laser-ablation techniques employing Mg atoms and acetylene molecules imply that following relaxation or decomposition, metastable excited Mg atoms can be inserted into the C–H bond of acetylene creating magnesaprop-2-yne (HCCMgH) [22]. Beyond this work, a binary complex consisting of Mg bound to acetylene has been theoretically studied at the BCCD(T)/6-311++G(3df,3pd) and MP2/6-311++G(3df,3pd) levels of theory and found to be in good agreement with experimental observation of a T-shaped or cyclic geometry for c-MgC_2H_2 [23] paving the way for potential observation of c-MgC_2H_2 if the proper spectral data can be measured.

Three isomers of the [Mg, C_2, H_2] complex including these above are reported using DFT at the B3LYP/6-311++G(2d,2p) and B3LYP-D3BJ/6-311++G(2d,2p) levels of theory along with CCSD(T)/aug-cc-pCVTZ [24]. Of these three low-lying isomers, magnesaprop-2-yne (HCCMgH), magnesapropadiene ($MgCCH_2$), and magnesacyclopropene (c-MgC_2H_2), the first and third have been previously reported; the second had not been as fully examined. Of these the most thermodynamically stable is the magnesaprop-2-yne isomer (HCCMgH) confirming earlier work. The ground state of the other two isomers, magnesapropadiene and magnesacyclopropene, is shown to be $1\,^3B_2$ as they both have C_{2v} symmetry. The triplet state of magnesapropadiene is more polar (1.290 D) than that of magnesacyclopropene (0.099 D). The higher-energy singlet electronic states of these C_{2v} molecules are more polar, 5.89 D and 5.25 D, respectively. Therefore, this theoretical previous study [24] asserts that the singlet HCCMgH isomer, while the lowest in energy, would be difficult to observe using microwave spectroscopy, but both triplet C_{2v} structures are highly probable foci for laboratory studies or astronomical observation [24].

The observation of c-MgC_2H_2 will require highly-accurate rotational constants and/or fundamental anharmonic vibrational frequencies depending upon the wavelength of light most fitting for the astronomical source observed. The use of fourth-order Taylor series approximations to the internuclear molecular Hamiltonian, or quartic force fields (QFFs), with high levels of quantum chemical electronic structure computations has been benchmarked to provide rotational constants typically within 0.12% of experiment for molecules of this size and fundamental anharmonic vibrational frequencies within 0.7% (roughly less than 6.0 cm^{-1}) [25–37]. Consequently, this study employs such quantum chemical approaches to produce the necessary rovibrational spectral data in order to characterize c-MgC_2H_2 in both its ground, triplet and excited, singlet state in order to assist potentially with its detection in the ISM. Finally, the possible formation mechanism for this molecule from acetylene and Mg will also be explored.

2. Computational methods

Unless otherwise noted, all computations make use of coupled cluster theory at the singles, doubles, and perturbative triples level [CCSD(T)] [38] within the explicitly correlated F12b formalism [39,40] and the cc-pVTZ-F12 basis set [41], henceforth abbreviated as F12-TZ, as available in the MOLPRO 2019.1 quantum chemistry program [42,43]. All computations for $1\,^3B_2$ c-MgC_2H_2 utilize restricted open-shell reference wave functions [44,45], while closed-shell molecules employ standard restricted Refs. [46].

All fundamental vibrational frequencies are generated through the use of QFFs in the fashion standard for these types of applications [25,26,47,48]. F12-TZ QFFs, specifically, are known to produce highly accurate vibrational frequencies at a relatively low computational cost

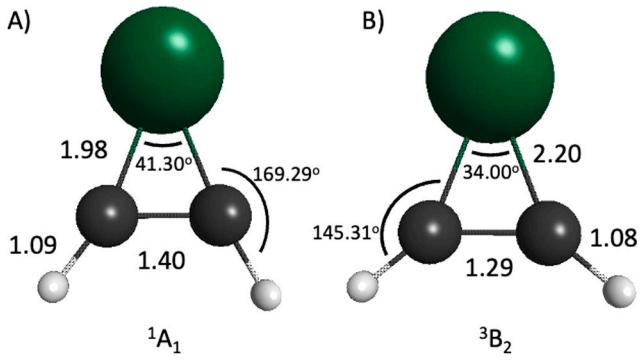

Fig. 1. A visual depiction of $1\,^1A_1$ (Structure A) and $1\,^3B_2$ (Structure B) of c-MgC_2H_2. Optimized bond lengths and angles are given in Å and degrees, respectively.

within 5 cm^{-1} or so of higher-order methods and even experimental results [49–51]. Regardless of electronic state, the geometries of both $1\,^1A_1$ and $1\,^3B_2$ c-MgC_2H_2 are first optimized with exceptionally tight convergence criteria. The reference geometry is displaced by 0.005 Å or 0.005 radians, respective of bond lengths and bond angles/dihedrals, using symmetry-internal coordinates via the INTDER program [52]. This molecule is of the same connectivity allowing for use of coordinates employed previously for similar cyclic species: cyclopropenylidene and its silanated analogue [36,53,54]. The coordinates are defined from Fig. 1 where the left-side of each structure should be understood to contain atoms C_1 and H_1 and vice versa:

$$S_1(a_1) = C_1 - C_2, \tag{1}$$

$$S_2(a_1) = \frac{1}{\sqrt{2}}[(Mg - C_1) + (Mg - C_2)], \tag{2}$$

$$S_3(a_1) = \frac{1}{\sqrt{2}}[(C_1 - H_1) + (C_2 - H_2)], \tag{3}$$

$$S_4(a_1) = \frac{1}{\sqrt{2}}\angle[(H_1 - C_1 - Mg) + (H_2 - C_2 - Mg)], \tag{4}$$

$$S_5(b_2) = \frac{1}{\sqrt{2}}[(Mg - C_1) - (Mg - C_2)], \tag{5}$$

$$S_6(b_2) = \frac{1}{\sqrt{2}}[(C_1 - H_1) - (C_2 - H_2)], \tag{6}$$

$$S_7(b_2) = \frac{1}{\sqrt{2}}\angle[(H_1 - C_1 - Mg) - (H_2 - C_2 - Mg)], \tag{7}$$

$$S_8(b_1) = \frac{1}{\sqrt{2}}\tau[(H_1 - C_1 - Mg - C_2) - (H_2 - C_2 - Mg - C_1)], \tag{8}$$

$$S_9(a_2) = \frac{1}{\sqrt{2}}\tau[(H_1 - C_1 - Mg - C_2) + (H_2 - C_2 - Mg - C_1)]. \tag{9}$$

Once the 1585 points for either electronic state are computed, their relative energies are fit via a least squares method to better than 10^{-17} a.u.[2] The generated force constants are then transformed from symmetry-internal coordinates into Cartesian coordinates using INTDER [52] as this is more computationally expedient for use in subsequent steps. The SPECTRO [55] program then computes the spectroscopic constants and vibrational frequencies, which are produced by rotational and vibrational perturbation theory at second order

(VPT2) [56–58]. The dipole moments for both 1 $^1A_1$ and 1 $^3B_2$ c-MgC_2H_2 are computed via F12-TZ using version 2020.1 of the MOLPRO quantum chemistry program [59] using finite differences of energies in response to an external electric field. Harmonic intensities for both electronic excited states are computed using Gaussian16 via the MP2/6-31+G(d) level of theory [60–62] which has been shown to produce semi-quantitative agreement with higher levels of theory for far less computational cost [63,64].

The rovibrational spectra of both 1 $^1A_1$ and 1 $^3B_2$ c-MgC_2H_2 contain Fermi resonances and polyads of these resonances that the SPECTRO program is capable of treating for more accurate predictions [65]. The 1 $^1A_1$ state of c-MgC_2H_2 contains a $\nu_8 + \nu_6 = 2\nu_7 = 2\nu_8 = 2\nu_9 = \nu_3$ polyad, another $2\nu_8 = 2\nu_9 = \nu_5$ polyad, a $\nu_9 + \nu_8 = \nu_4$ type-2 Fermi resonance, and multiple Coriolis resonances: a ν_5/ν_4 A-type, a ν_6/ν_4 B-type, a ν_8/ν_7 C-type, and a ν_9/ν_8 A-type. The 1 $^3B_2$ state of c-MgC_2H_2 contains a $2\nu_3 = \nu_1$ and $2\nu_9 = \nu_8$ type-1 Fermi resonances, $2\nu_4 = 2\nu_5 = \nu_3$ and $2\nu_8 = 2\nu_9 = \nu_4$ polyads, a $\nu_9 + \nu_7 = \nu_6$ and $2\nu_9 + \nu_8 = \nu_5$ type-2 Fermi resonances, and multiple Coriolis resonances: a ν_6/ν_4 A-type, a ν_6/ν_5 B-type, and a ν_9/ν_8 C-type.

In order to examine how this molecule may form in the ISM such that it can be observed in the first place, relaxed scans of both the lowest singlet and triplet electronic states of Mg + C_2H_2 are undertaken. The association of Mg atoms to acetylene is modeled by varying the distance between the Mg atom to the midpoint of the C–C bond in acetylene denoted as point X. Mg–X distances are varied from 1.65 Bohr to 5.55 Bohr with step sizes of 0.1 Bohr, and the ∠Mg–X–C angles are fixed at 90°. The remaining geometrical parameters are allowed to optimize at each Mg–X bond length allowing for a relaxed scan.

3. Results and discussion

3.1. Structural and rotational considerations of c-MgC_2H_2

The 1 $^3B_2$ state of magnesacyclopropene lies 10.28 kcal/mol (0.446 eV or 3596 cm^{-1}) below the 1 $^1A_1$ state including the anharmonic zero-point vibrational energy correction in line with previous prediction of 10.41 kcal/mol [24]. The orbital occupation for the ground 1 $^3B_2$ state is (core) $5a_1^2 3b_2^2 6b_1^2 7a_1^2 2b_1^2 4b_2^1 8a_1^1$. The singlet doubly occupies the $4b_2$ orbital in its wavefunction. The two highest occupied molecular orbitals (MOs) in the singlet state represent the two π orbitals of acetylene. The additional, highest singly-occupied MO of the 1 $^3B_2$ state is a majority non-bonding/lone-pair-type orbital on the Mg atom opposite the acetylene.

The optimized F12-TZ equilibrium singlet and triplet state Mg–C bond lengths are 1.98 Å and 2.20 Å, respectively, along with H–C bond lengths that are nearly equivalent at 1.09 Å and 1.08 Å, respectively. The C-Mg-C angle is shown to be 41.3 and 34.0 degrees, respectively. Interestingly, the largest structural difference between these two electronic states lies with the ∠H–C–Mg angle. The triplet state has a bond angle of 145.3°, roughly 25° less than that of the singlet state given in Table 1. Consequently, when the electron is excited, this angle begins to relax displaying a more acetylenic structure.

Additionally, the structural changes, especially the C=C bond length as shown in Fig. 1 and listed in Table 1, are attributable to different occupations of the electrons, as well. From Fig. 2, the highest occupied molecular orbital ($4b_2$) of the 1 $^1A_1$ state has repulsion between the two carbon atoms leading to a longer C = C bond at 1.40 Å than the 1.29 Å C = C bond in the 1 $^3B_2$. Once this orbital is only singly-occupied in the triplet state with one electron moving into the $8a_1$ orbital (also in Fig. 2), the repulsion decreases allowing this bond to shorten. Furthermore, the C-Mg-C angle relaxes from 41.30° to 34.00°, the H-C-Mg angle decreases from 169.29° to 145.31°, and the Mg-C bond lengthens from 1.98 Å to 2.20 Å. The electron repulsion is also, again, likely the probable cause for the H-C-Mg angle being greater in the 1 $^1A_1$ state.

Table 1
Geometries and spectroscopic constants for $^1A_1$ and $^3B_2$ electronic states of c-MgC_2H_2 compared to previous theory[a].

		1 $^1A_1$ c-MgC_2H_2		1 $^3B_2$ c-MgC_2H_2	
	Units	F12-TZ	Previous theory	F12-TZ	Previous theory
R_e(Mg–C)	Å	1.97873	1.9717	2.19761	2.1871
R_e(C–C)	Å	1.39522	1.3979	1.28433	1.2865
R_e(C–H)	Å	1.09360	1.0937	1.08448	1.0848
$\angle_e$(C–Mg–C)	°	41.29	41.52	33.98	34.21
$\angle_e$(Mg–C–H)	°	169.27	169.30	145.28	145.42
A_e	MHz	33 883.9	33 750.97	35 115.4	35 021.38
B_e	MHz	10 568.5	10 655.49	8605.3	8695.03
C_e	MHz	8055.9	8098.67	6911.6	6965.62
R_0(Mg–C)	Å	1.99680		2.20956	
R_0(C–C)	Å	1.39605		1.28884	
R_0(C–H)	Å	1.09392		1.08099	
$\angle_0$(C–Mg–C)	°	40.92		33.91	
$\angle_0$(Mg–C–H)	°	168.31		145.32	
A_0	MHz	33 816.9		35 066.4	
B_0	MHz	10 403.1		8545.0	
C_0	MHz	7939.9		6851.1	
A_1	MHz	33 774.2		34 958.1	
B_1	MHz	10 376.6		8533.0	
C_1	MHz	7922.1		6839.2	
A_2	MHz	33 792.0		34 971.2	
B_2	MHz	10 375.4		8532.4	
C_2	MHz	7922.4		6839.5	
A_3	MHz	33 546.1		34 825.3	
B_3	MHz	10 420.9		8546.8	
C_3	MHz	7934.1		6842.8	
A_4	MHz	33 677.7		35 170.7	
B_4	MHz	10 396.9		8563.4	
C_4	MHz	7938.6		6847.3	
A_5	MHz	33 799.3		35 256.2	
B_5	MHz	10 420.4		8561.4	
C_5	MHz	7937.2		6855.0	
A_6	MHz	34 260.4		34 994.5	
B_6	MHz	10 226.1		8545.3	
C_6	MHz	7835.0		6854.0	
A_7	MHz	33 808.2		34 858.2	
B_7	MHz	10 358.2		8522.0	
C_7	MHz	7900.7		6857.0	
A_8	MHz	33 978.6		35 066.4	
B_8	MHz	10 344.3		8490.6	
C_8	MHz	7893.2		6811.9	
A_9	MHz	33 582.0		35 399.4	
B_9	MHz	10 378.9		8489.8	
C_9	MHz	7943.7		6792.8	
Δ_J	kHz	8.117	8.233	9.305	9.411
Δ_K	kHz	68.764	−68.700	−65.998	−69.100
Δ_{JK}	kHz	42.128	−41.800	146.621	149.333
δ_J	kHz	1.990	2.035	1.924	1.965
δ_K	kHz	37.423	37.400	94.756	96.200
Φ_J	mHz	2.267		2.034	
Φ_K	Hz	−0.302		−6.369	
Φ_{JK}	mHz	−9.215		−496.097	
Φ_{KJ}	Hz	0.640		7.399	
ϕ_J	mHz	1.709		2.260	
ϕ_{JK}	mHz	−15.836		263.945	
ϕ_K	Hz	2.477		18.856	
μ	D	5.47.	5.2480	0.11	0.0988

[a]Ref. [24].

These structural parameters produce rotational constants that display some prolate character with the B and C constants of the singlet state being larger than their triplet counterparts. The currently computed equilibrium geometrical values and rotational constants are also in good agreement with previous work [24]. However, Table 1 also provides the sextic distortion constants, the vibrationally-averaged (R_α) rotational constants (including A_0, B_0, and C_0 constants), and the vibrationally-excited rotational constants for the ^{24}Mg isotope that are numbered in the same order as the fundamental vibrational frequencies given in Table 2. The comparison of the dipole moments for the two electronic states examined presently, found in Table 1, corroborate the

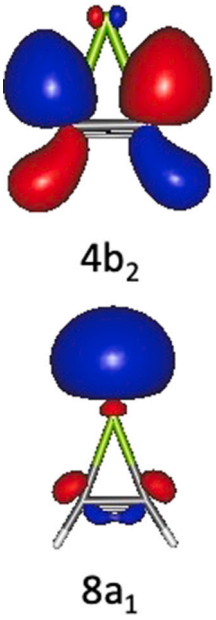

Fig. 2. A visual depiction of the $4b_2$ and $8a_1$ MOs of $1\ ^1A_1$ *c*-MgC_2H_2.

previous disparity in the dipole moments with the $1\ ^3B_2$ state's mere 0.11 D falling shockingly short of the $1\ ^1A_1$ state's much larger 5.47 D. This disproportion can be attributed to the partial charge of Mg and the electron density in each state. In the $1\ ^1A_1$ state, the partial charge of Mg is 0.64, while 0.38 in the $1\ ^3B_2$ state. Finally, the ^{25}Mg, ^{26}Mg, and D isotopologue data are giving in the supplemental information (SI).

3.2. Vibrational analysis data for c-MgC_2H_2

The $1\ ^3B_2$ electronic state is shown to be the ground electronic state in Fig. 3, and contains a high intensity vibrational mode of 118 km/mol (as shown in Table 2) for the ω_8 mode with a corresponding ν_8 frequency of 513.5 cm^{-1}. While this mode may be highly observable given the large intensity value, the $1\ ^1A_1$ electronic state contains an even higher intensity mode, the ω_6 mode, at 276 km/mol with a corresponding ν_6 frequency at 827.8 cm^{-1}. Additionally, the $1\ ^1A_1$ state has three fundamentals with intensities above 100 km/mol in line with similar Mg-bearing molecules computed recently [66] while the $1\ ^3B_2$ state only contains one mode with an intensity above 100 km/mol. The $1\ ^1A_1$ state is more tightly bound to its magnesium atom, as discussed in the next section and as evidenced by the nearly doubled F_{22} force constant in the singlet state as given in Tables S1 and S2 in the SI. As such, the intensity of the $1\ ^1A_1$ frequencies will be influenced by the bonding while the Mg atom of the $1\ ^3B_2$ state will have significantly less influence on the induced dipole moments of this state. For both electronic states, a larger number of fundamental frequencies fall into the sub-1000 cm^{-1} regime as compared to most *p*-block molecules due to the heavier mass of and weaker bonding to the magnesium atom.

Overall, the F12-TZ harmonic frequencies for the $1\ ^1A_1$ and $1\ ^3B_2$ state of c-MgC_2H_2 compare well with previous theory with the best agreement being less than 0.5 cm^{-1} for the $1\ ^3B_2$ ω_7 mode [24] as shown in Table 2. The worst agreement between previous and present theory is approximately 31 cm^{-1} for the $1\ ^1A_1$ ω_6 mode. This, however, is less than 5% and is within the accepted margin of error. This analysis implies that the present study's F12-TZ QFF vibrational frequency data are accurate and reliable. However, the present study goes beyond merely the harmonic frequencies to, again, produce the anharmonic fundamental frequencies as given in Table 2.

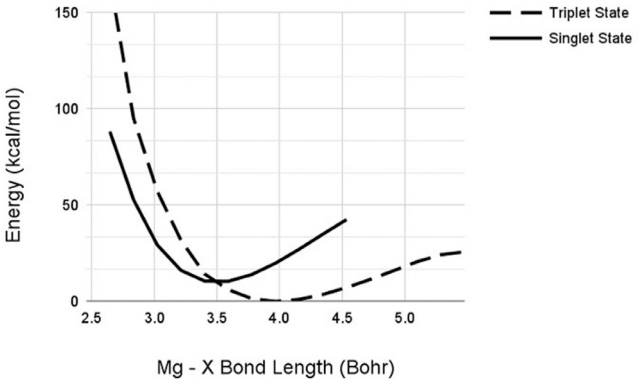

Fig. 3. The Mg–X scan for both the $1\ ^3B_2$ and $1\ ^1A_1$ states of c-MgC_2H_2.

3.3. Formation of c-MgC_2H_2

The present work proposes two possible mechanisms for the formation of $1\ ^3B_2$ c-MgC_2H_2 that conserves spin:

$$Mg(^3P_2) + 1\ ^1A_1\ C_2H_2 \rightarrow 1\ ^3B_2\ MgC_2H_2 \tag{10}$$

$$Mg(^1S_0) + 1\ ^3\Sigma_u^+\ C_2H_2 \rightarrow 1\ ^3B_2\ MgC_2H_2 \tag{11}$$

In Eq. (10), C_2H_2 remains in its ground electronic state. The computed singlet-to-triplet excitation energy for Mg at the F12-TZ level is 59.84 kcal/mol (2.59 eV). Conversely, in Eq. (11), Mg would remain in the ground electronic state with the calculated excitation energy for C_2H_2 lying 115.84 kcal/mol (5.02 eV), almost double that of Mg. This is not surprising given that the bond order in acetylene must be reduced during such an excitation. Hence, the excitation of the Mg atom is more likely to contribute to the formation of $1\ ^3B_2$ c-MgC_2H_2 as is borne out in the triplet dissociation in Fig. 3. However, an intersystem crossing from the $1\ ^3B_2$ state could still form the $1\ ^1A_1$ state.

Both the singlet and triplet PES for the Mg–X relaxed scan of the C_{2v} isomer of c-MgC_2H_2 are depicted in Fig. 3. Both clearly exhibit Morse potentials with the triplet state being flatter than the singlet. Previous work has been conducted for protonated acetylene, which shares comparable connectivity and ligand-acetylene core interactions, exhibiting a flat PES. The results of the QFF analysis for this molecule shows agreement between the computed and experimental values to better than 0.1% implying that the current methodology produces accurate descriptions of such flat surfaces [31]. The triplet dissociation energy is 41.03 kcal/mol while the singlet is higher at 94.89 kcal/mol (relative to its own minimum) in line with roughly half the Mg–C bond strength in the comparable $HMgCH_3$ molecule [67]. The optimal Mg–X bond length for the $1\ ^3B_2$ is determined to be 2.10 Å and 1.90 Å in the singlet state for this scan.

The flat PES for the triplet surface brings the vibrational levels closer together for what is effectively the S_2 coordinate and ν_4 fundamental in the Mg–X stretch. As such the descent through the vibrational levels could be enhanced in environments where the collision probability is relatively high. Additionally, the overlap between the two electronic states allows for a low energy excited state. The vertical $1\ ^1A_1 \leftarrow 1\ ^3B_2$ transition is computed on this scan to be 19.82 kcal/mol or 6932 cm^{-1}. Adjusting for the estimated ZPVE for ν_4 of roughly 224 cm^{-1} reduces this vertical excitation down to 6708 cm^{-1} or 1491 nm. Conversely, formation of the $1\ ^1A_1$ state could readily relax to the triplet surface due to the high degree of overlap as shown in Fig. 3. In either case, these two electronic states would likely coevolve to some degree implying that even if the triplet surface is preferred in Mg association with acetylene, formation of the singlet would have a relatively low energy cost if somewhat less likely pathway to access.

Table 2
Vibrational frequencies (cm^{-1}), and IR intensities (km/mol), given in parenthesis, for $^1A_1$ and $^3B_2$ electronic states of c-MgC_2H_2 compared to previous theory and experiment.

		$1\ ^1A_1$ c-MgC_2H_2			$1\ ^3B_2$ c-MgC_2H_2	
	Description[a]	F12-TZ	Previous theory[b]	Desc.[a]	F12-TZ	Previous theory[b]
$\omega_1(a_1)$	(S_3)	3055.6 (130)	3058.3 (134.0)	(S_3)	3168.0 (3)	3169.7 (5.6)
$\omega_2(a_1)$	(S_1)	1303.4 (12)	1298.89 (7.8)	(S_1)	1683.8 (5)	1679.5 (0.1)
$\omega_3(a_1)$	(S_4)	965.7 (1)	970.4 (0.7)	(S_4)	809.0 (7)	810.0 (8.1)
$\omega_4(a_1)$	(S_2)	647.2 (14)	649.9 (6.9)	(S_2)	463.1 (58)	467.0 (54.3)
$\omega_5(b_2)$	(S_6)	3027.1 (44)	3028.4 (39.1)	(S_6)	3123.9 (1)	3119.7 (88.6)
$\omega_6(b_2)$	$0.56(S_7)-0.44(S_5)$	827.8 (276)	797.1 (208.7)	(S_7)	765.5 (17)	762.4 (81.5)
$\omega_7(b_2)$	$0.56(S_5)+0.44(S_7)$	573.3 (8)	564.7 (6.2)	(S_5)	325.1 (67)	324.8 (0.3)
$\omega_8(b_1)$	(S_8)	568.2 (212)	571.3 (157.9)	(S_8)	513.5 (118)	517.4 (89.9)
$\omega_9(a_2)$	(S_9)	1010.0 (-)	1008.3 (-)	(S_9)	732.1 (-)	738.8 (0)
$\nu_1(a_1)$	(S_3)	2901.9		(S_3)	3005.3	
$\nu_2(a_1)$	(S_1)	1259.5		(S_1)	1649.1	
$\nu_3(a_1)$	(S_4)	932.9		(S_4)	775.6	
$\nu_4(a_1)$	(S_2)	580.0		(S_2)	447.9	
$\nu_5(b_2)$	(S_6)	2873.5		(S_6)	2962.3	
$\nu_6(b_2)$	$0.56(S_7)-0.44(S_5)$	648.4		(S_7)	739.5	
$\nu_7(b_2)$	$0.56(S_5)+0.44(S_7)$	525.6		(S_5)	312.8	
$\nu_8(b_1)$	(S_8)	531.8		(S_9)	720.7	
$\nu_9(a_2)$	(S_9)	971.2		(S_8)	500.5	
ZPT		5840.4			5706.3	

[a]Contributes more than 90% to the dominant components of a coordinate unless specified otherwise.
[b]Previous theory for $1\ ^1A_1$ utilizes ae-CCSD(T)/aug-cc-pCVTZ, and $1\ ^3B_2$ utilizes ae-ROCCSD(T)/aug-cc-pCVTZ from Ref. [24].

Radiative association (RA) appears to be the lowest energy mechanism for any gas phase formation of c-MgC_2H_2. Several attempts to compute reaction schema for known Mg-containing interstellar molecules with acetylene returned high barriers as well as thermodynamically and kinetically disfavorable results. Mostly, the Mg–C bond energy of c-MgC_2H_2 is weaker than the Mg–C and Mg–N bonds of known interstellar molecules. While RA is notoriously slow in the gas phase, c-MgC_2H_2 has underlying properties that may increase the likelihood of observation for the more intense rotational and vibrational transitions of the $1\ ^1A_1$ state.

4. Conclusions

The more intense vibrational transitions and the larger dipole moment imply that the $1\ ^1A_1$ state of c-MgC_2H_2 is the more likely candidate than the $1\ ^3B_2$ state for potential observation by the *James Webb Space Telescope* in the infrared and also for radioastronomical spectroscopic observation from the ground. The 5.47 D dipole moment for the $1\ ^1A_1$ state of c-MgC_2H_2 will be more observable than its lower-lying $1\ ^3B_2$ counterpart (0.11 D) in the submillimeter regime. While the two states are more similar in their infrared intensities, the singlet state has three fundamentals with intensities above 100 km/mol while the triplet has only one. Additionally, the formation of this molecule appears to require radiative association, but the relatively flat triplet PES likely facilitates faster association of the triplet state than most cases invoking RA and both states will likely coevolve due to the relative low energy separating them along the Mg–X coordinate. In any case, the spectral data provided in this work will no doubt assist with any potential laboratory observations of this molecule paving the way for possible later astronomical observation.

CRediT authorship contribution statement

Kimberley N. Poland: Conceptualization, Methodology, Validation, Formal analysis, Investigation, Writing – original draft, Writing – review & editing, Visualization, Supervision. **C. Zachary Palmer:** Conceptualization, Methodology, Validation, Formal analysis, Investigation, Writing – original draft, Writing – review & editing, Visualization. **Ava Chard:** Formal analysis, Investigation, Writing – review & editing. **Steven R. Davis:** Validation, Formal analysis, Writing – review & editing. **Ryan C. Fortenberry:** Conceptualization, Methodology, Software, Validation, Formal analysis, Resources, Writing – original draft, Writing – review & editing, Visualization, Supervision, Project administration, Funding acquisition.

Declaration of competing interest

The authors declare that they have no known competing financial interests or personal relationships that could have appeared to influence the work reported in this paper.

Acknowledgments

The authors wish to acknowledge funding from NASA grant NNX17AH15G, NSF Grant CHE-1954922, start-up funds provided by the University of Mississippi, and computing resources provided by the Mississippi Center for Supercomputing Research funded in part by NSF Grants CHE-1338056 and OIA-1757220. Additionally, this work was also supported by NSF REU grant CHE-1757888.

Appendix. Supplementary data

Supplementary material related to this article can be found online at https://doi.org/10.1016/j.jms.2021.111514. The supplementary information includes the force constants for the $1\ ^1A_1$ and $1\ ^3B_2$ states of c-MgC_2H_2, respectively shown in Tables S1 and S2. These are provided by the INTDER program that are then used by SPECTRO to compute the harmonic and anharmonic frequencies included in this work. Additionally, Tables S3 and S5 provide harmonic and fundamental anharmonic frequencies for c-$^{25}MgC_2H_2$ and c-$^{26}MgC_2H_2$ as well as c-MgC_2HD and c-MgC_2D_2, respectively. Tables S4 and S6 provide geometrical parameters as well as the quartic and sextic distortion constants, the vibrationally-averaged (R_a) rotational constants, and the vibrationally-excited rotational constants for the, respective, aforementioned isotopologues of c-MgC_2H_2.

References

[1] L. Snyder, Interferometric observations of large biologically interesting interstellar and cometary molecules, Proc. Natl. Acad. Sci. 103 (2006) 12243–12248.
[2] E. Herbst, W. Klemperer, The formation and depletion of molecules in dense interstellar clouds, Astrophys. J. 185 (1973) 505–533.
[3] E. Herbst, C.E. M., Monte Carlo studies of surface chemistry and nonthermal desorption involving interstellar grains, Proc. Natl. Acad. Sci. 103 (2006) 12257–12262.

[4] B.H. Mahan, Electronic structure and chemical dynamics, Acc. Chem. Res. 8 (1975) 55–61.

[5] L. Ziurys, The chemistry in circumstellar envelopes of evolved stars: Following the origin of the elements to the origin of life, Proc. Natl. Acad. Sci. 103 (2006) 12274–12279.

[6] F.C. Fehsenfeld, A.L. Schmeltekopf, P.D. Golden, H.I. Schiff, E.E. Ferguson, Thermal energy ion-neutral rates. I. Some reactions of helium ions, J. Chem. Phys. 44 (1966) 4087–4094.

[7] W. Klemperer, Interstellar chemistry, Proc. Natl. Acad. Sci. 103 (2006) 12232–12234.

[8] B.A. McGuire, A.M. Burkhardt, S. Kalenskii, C.N. Shingledecker, A.J. Remijan, E. Herbst, M.C. McCarthy, Detection of the aromatic molecule benzonitrile (c-C_6H_5CN) in the interstellar medium, Science 359 (2018) 202–205.

[9] J.H. Lacy, N.J. Evans II, J.M. Achtermann, D.E. Bruce, Discovery of interstellar acetylene, Astrophys. J. 342 (1989) 43–46.

[10] B.A. McGuire, 2018 census of interstellar, circumstellar, extragalactic, protoplanetary disk, and exoplanetary molecules, Astrophys. J. Suppl. Ser. 239 (2018) 17.

[11] R.C. Fortenberry, The case for gas-phase astrochemistry without carbon, Mol. Astrophys. 18 (2020) 100062.

[12] J. Cernicharo, C. Cabezas, J.R. Pardo, M. Agúndez, C. Bermúdez, L. Velilla-Prieto, F. Tercero, J.A. López-Pérez, J.D. Gallego, J.P. Fonfría, G. Quintana-Lacaci, M. Guélin, Y. Endo, Discovery of two new magnesium-bearing species in IRC+10216: MgC_3N and MgC_4H, Astron. Astrophys. 630 (2019) L2.

[13] C.Z. Palmer, R.C. Fortenberry, Rovibrational considerations for the monomers and dimers of magnesium hydride (MgH_2) and magnesium fluoride (MgF_2), J. Phys. Chem. A 122 (2018) 7079–7088.

[14] K. Kawaguchi, E. Kagi, T. Hirano, S. Takano, S. Saito, Laboratory spectroscopy of MgNC: First radioastronomical identification of a Mg-bearing molecule, Astrophys. J. 406 (1993) L39–L42.

[15] V.Z. Adibekyan, N.C. Santos, S.G. Sousa, E.D. Mena, J.I.G. Hernández, M. Mayor, C. Lovis, S. Udrys, Overabundance of α-elements in exoplanets-hosting stars, Astron. Astrophys. 543 (2012) A89.

[16] V. Adibekyan, N.C. Santos, P. Figueira, C. Dorn, S.G. Sousa, E. Delgado-Mena, G. Israelian, A.A. Hakobyan, C. Mordasini, From stellar to planetary composition: Galactic chemical evolution of Mg/Si mineralogical ratio, Astron. Astrophys. 581 (2015) L2.

[17] C.M. Mauney, D. Lazzati, The formation of astrophysical mg-rich silicate dust, Mol. Astrophys. 12 (2018) 1–9.

[18] L.M. Ziurys, A.J. Apponi, M. Guélin, J. Cernicharo, Detection of MgCN in IRC +10216: A new metal-bearing free radical, Astrophys. J. 445 (1995) L47–L50.

[19] M. Agúndez, J. Cernicharo, M. Guélin, New molecules in IRC +10216: Confirmation of C_5S and tentative identification of MgCCH, NCCP, and SiH_3CN, Aston. Astrophys. 570 (2014) A45.

[20] B.A. McGuire, P.B. Carroll, R.A. Loomis, I.A. Finneran, P.R. Jewell, A.J. Remijan, G.A. Blake, Discovery of the interstellar chiral molecule propylene oxide (CH_3CHCH_2O), Science 352 (2016) 1449–1452.

[21] J.R. Flores, A. Largo, Theoretical study of the interactions of beryllium and magnesium atoms with acetylene, J. Phys. Chem. 95 (1991) 9278–9288.

[22] C.A. Thompson, L. Andrews, Reactions of laser-ablated be and Mg atoms with C_2H_2: Infrared spectra and density functional calculations of novel metal-acetylene species, J. Am. Chem. Soc. 118 (1996) 10242–10249.

[23] D.T. Moore, R.E. Miller, Structure of the acetylene-magnesium binary complex from infrared laser spectroscopy in helium nanodroplets, J. Phys. Chem. A 108 (2004) 9908–9915.

[24] V.S. Thimmakondu, MgC_2H_2 isomers - simple penta-atomic molecules missing in the laboratory, J. Chem. Phys. 538 (2020).

[25] X. Huang, T.J. Lee, A procedure for computing accurate *ab initio* quartic force fields: Application to HO_2^+ and H_2O, J. Chem. Phys. 129 (2008) 044312.

[26] X. Huang, T.J. Lee, Accurate *Ab Initio* quartic force fields for NH_2^- and CCH^- and rovibrational spectroscopic constants for their isotopologs, J. Chem. Phys. 131 (2009) 104301.

[27] X. Huang, P.R. Taylor, T.J. Lee, Highly accurate quartic force field, vibrational frequencies, and spectroscopic constants for cyclic and linear $C_3H_3^+$, J. Phys. Chem. A 115 (2011) 5005–5016.

[28] D. Zhao, K.D. Doney, H. Linnartz, Laboratory gas-phase detection of the cyclopropenyl cation (c-$C_3H_3^+$), Astrophys. J. Lett. 791 (2014) L28.

[29] R.C. Fortenberry, X. Huang, J.S. Francisco, T.D. Crawford, T.J. Lee, Quartic force field predictions of the fundamental vibrational frequencies and spectroscopic constants of the cations $HOCO^+$ and $DOCO^+$, J. Chem. Phys. 136 (2012) 234309.

[30] X. Huang, R.C. Fortenberry, T.J. Lee, Protonated nitrous oxide, $NNOH^+$: Fundamental vibrational frequencies and spectroscopic constants from quartic force fields, J. Chem. Phys. 139 (8) (2013) 084313.

[31] R.C. Fortenberry, X. Huang, T.D. Crawford, T.J. Lee, Quartic force field rovibrational analysis of protonated acetylene, $C_2H_3^+$, and its isotopologues, J. Phys. Chem. A 118 (2014) 7034–7043.

[32] R.C. Fortenberry, T.J. Lee, H.S.P. Müller, Excited vibrational level rotational constants for SiC_2: A sensitive molecular diagnostic for astrophysical conditions, Mol. Astrophys. 1 (2015) 13–19.

[33] M.J.R. Kitchens, R.C. Fortenberry, The rovibrational nature of closed-shell third-row triatomics: HOX and HXO, X=Si^+, P, S^+, and Cl, Chem. Phys. 472 (2016) 119–127.

[34] L. Bizzocchi, V. Lattanzi, J. Laas, S. Spezzano, B.M. Giuliano, D. Prudenzano, C. Endres, O. Sipilä, P. Caselli, Accurate sub-millimetre rest frequencies for $HOCO^+$ and $DOCO^+$ ions, Astron. Astrophys. 602 (2017) A34.

[35] R.C. Fortenberry, Quantum astrochemical spectroscopy, Int. J. Quantum Chem. 117 (2017) 81–91.

[36] R.C. Fortenberry, C.M. Novak, J.P. Layfield, E. Matito, T.J. Lee, Overcoming the failure of correlation for out-of-plane motions in a simple aromatic: Rovibrational quantum chemical analysis of c-C_3H_2, J. Chem. Theor. Comput. 14 (2018) 2155–2164.

[37] M.B. Gardner, B.R. Westbrook, R.C. Fortenberry, T.J. Lee, Highly-accurate quartic force fields for the prediction of anharmonic rotational constants and fundamental vibrational frequencies, Spectrochim. Acta A 248 (2021) 119184.

[38] K. Raghavachari, G.W. Trucks, J.A. Pople, M. Head-Gordon, A fifth-order perturbation comparison of electron correlation theories, Chem. Phys. Lett. 157 (1989) 479–483.

[39] T.B. Adler, G. Knizia, H.-J. Werner, A simple and efficient CCSD(T)-F12 approximation, J. Chem. Phys. 127 (2007) 221106.

[40] G. Knizia, T.B. Adler, H.-J. Werner, Simplified CCSD(T)-F12 methods: Theory and benchmarks, J. Chem. Phys. 130 (2009) 054104.

[41] K.A. Peterson, T.B. Adler, H.-J. Werner, Systematically convergent basis sets for explicitly correlated wavefunctions: The atoms H, He, B-Ne, and Al-Ar, J. Chem. Phys. 128 (2008) 084102.

[42] H.-J. Werner, P.J. Knowles, G. Knizia, F.R. Manby, M. Schütz, P. Celani, W. Györffy, D. Kats, T. Korona, R. Lindh, A. Mitrushenkov, G. Rauhut, K.R. Shamasundar, T.B. Adler, R.D. Amos, S.J. Bennie, A. Bernhardsson, A. Berning, D.L. Cooper, M.J.O. Deegan, A.J. Dobbyn, F. Eckert, E. Goll, C. Hampel, A. Hesselmann, G. Hetzer, T. Hrenar, G. Jansen, C. Köppl, S.J.R. Lee, Y. Liu, A.W. Lloyd, Q. Ma, R.A. Mata, A.J. May, S.J. McNicholas, W. Meyer, T.F. Miller III, M.E. Mura, A. Nicklass, D.P. O'Neill, P. Palmieri, D. Peng, K. Pflüger, R. Pitzer, M. Reiher, T. Shiozaki, H. Stoll, A.J. Stone, R. Tarroni, T. Thorsteinsson, M. Wang, M. Welborn, MOLPRO, version 2019.2, a package of ab initio programs, 2019, see http://www.molpro.net.

[43] H.-J. Werner, P.J. Knowles, G. Knizia, F.R. Manby, M. Schütz, Molpro: A general-purpose quantum chemistry program package, WIREs Comput. Mol. Sci. 2 (2012) 242–253.

[44] J.S. Brinkley, J.A. Pople, P.S. Dobosh, Mol. Phys. 28 (1974) 1423–1429.

[45] J.D. Watts, J. Gauss, R.J. Bartlett, Coupled-cluster methods with noniterative triple excitations for restricted open-shell hartree-fock and other general single determinant reference functions. Energies and analytical gradients, J. Chem. Phys. 98 (1993) 8718–8733.

[46] A.C. Scheiner, G.E. Scuseria, J.E. Rice, T.J. Lee, H.F. Schaefer III, Analytic evaluation of energy gradients for the single and double excitation coupled cluster (CCSD) wave function: Theory and application, J. Chem. Phys. 87 (7) (1987) 5361–5373.

[47] R.C. Fortenberry, X. Huang, J.S. Francisco, T.D. Crawford, T.J. Lee, The *trans*-HOCO radical: Fundamental vibrational frequencies, quartic force fields, and spectroscopic constants, J. Chem. Phys. 135 (2011) 134301.

[48] R.C. Fortenberry, T.J. Lee, Computational vibrational spectroscopy for the detection of molecules in space, Annu. Rep. Comput. Chem. 15 (2019) 173–202.

[49] D. Agbaglo, T.J. Lee, R. Thackston, R.C. Fortenberry, A small molecule with PAH vibrational properties and a detectable rotational spectrum: c-$(C)C_3H_2$, cyclopropenylidenyl carbene, Astrophys. J. 871 (2019) 236.

[50] D. Agbaglo, R.C. Fortenberry, The performance of CCSD(T)-F12/aug-cc-pVTZ for the computation of anharmonic fundamental vibrational frequencies, Int. J. Quantum Chem. 119 (2019) e25899.

[51] D. Agbaglo, R.C. Fortenberry, The performance of explicitly correlated wavefunctions [CCSD(T)-F12b] in the computation of anharmonic vibrational frequencies, Chem. Phys. Lett. 734 (2019) 136720.

[52] W.D. Allen, et al., *INTDER* 2005 Is a general program written by W. D. Allen and Coworkers, which performs vibrational analysis and higher-order non-linear transformations, 2005.

[53] R.C. Fortenberry, T.J. Lee, J.P. Layfield, Communication: The failure of correlation to describe carbon=carbon bonding in out-of-plane bends, J. Chem. Phys. 147 (2017) 221101.

[54] R.C. Fortenberry, C.M. Novak, T.J. Lee, Rovibrational analysis of *c*-SiC_2H_2: Further evidence for out-of-plane bending issues in correlated methods, J. Chem. Phys. 149 (2018) 024303.

[55] J.F. Gaw, A. Willets, W.H. Green, N.C. Handy, in: J.M. Bowman, M.A. Ratner (Eds.), Advances in Molecular Vibrations and Collision Dynamics, JAI Press, Inc., Greenwich, CT, 1991.

[56] I.M. Mills, Vibration-rotation structure in asymmetric- and symmetric-top molecules, in: K.N. Rao, C.W. Mathews (Eds.), Molecular Spectroscopy - Modern Research, Academic Press, New York, 1972, pp. 115–140.

[57] D. Papousek, M.R. Aliev, Molecular Vibration-Rotation Spectra, Elsevier, Amsterdam, 1982.

[58] J.K.G. Watson, Aspects of quartic and sextic centrifugal effects on rotational energy levels, in: J.R. During (Ed.), Vibrational Spectra and Structure, Elsevier, Amsterdam, 1977, pp. 1–89.

[59] H.-J. Werner, P.J. Knowles, F.R. Manby, J.A. Black, K. Doll, A. Heßelmann, D. Kats, A. Köhn, T. Korona, D.A. Kreplin, Q. Ma, T.F. Miller III, A. Mitrushchenkov, K.A. Peterson, I. Polyak, G. Rauhut, M. Sibaev, Molpro, version 2020.1, a package of ab initio programs, 2020, see http://www.molpro.net.

[60] C. Møller, M.S. Plesset, Note on an approximation treatment for many-electron systems, Phys. Rev. 46 (1934) 618–622.

[61] W.J. Hehre, R. Ditchfeld, J.A. Pople, Self-consistent molecular orbital methods. XII. Further extensions of Gaussian-type basis sets for use in molecular orbital studies of organic molecules, J. Chem. Phys. 56 (1972) 2257.

[62] M.J. Frisch, G.W. Trucks, H.B. Schlegel, G.E. Scuseria, M.A. Robb, J.R. Cheeseman, G. Scalmani, V. Barone, G.A. Petersson, H. Nakatsuji, X. Li, M. Caricato, A.V. Marenich, J. Bloino, B.G. Janesko, R. Gomperts, B. Mennucci, H.P. Hratchian, J.V. Ortiz, A.F. Izmaylov, J.L. Sonnenberg, D. Williams-Young, F. Ding, F. Lipparini, F. Egidi, J. Goings, B. Peng, A. Petrone, T. Henderson, D. Ranasinghe, V.G. Zakrzewski, J. Gao, N. Rega, G. Zheng, W. Liang, M. Hada, M. Ehara, K. Toyota, R. Fukuda, J. Hasegawa, M. Ishida, T. Nakajima, Y. Honda, O. Kitao, H. Nakai, T. Vreven, K. Throssell, J.A. Montgomery Jr., J.E. Peralta, F. Ogliaro, M.J. Bearpark, J.J. Heyd, E.N. Brothers, K.N. Kudin, V.N. Staroverov, T.A. Keith, R. Kobayashi, J. Normand, K. Raghavachari, A.P. Rendell, J.C. Burant, S.S. Iyengar, J. Tomasi, M. Cossi, J.M. Millam, M. Klene, C. Adamo, R. Cammi, J.W. Ochterski, R.L. Martin, K. Morokuma, O. Farkas, J.B. Foresman, D.J. Fox, Gaussian 16 Revision C.01, Gaussian Inc., Wallingford CT, 2016.

[63] Q. Yu, J.M. Bowman, R.C. Fortenberry, J.S. Mancini, T.J. Lee, T.D. Crawford, W. Klemperer, J.S. Francisco, The structure, anharmonic vibrational frequencies, and intensities of $NNHNN^+$, J. Phys. Chem. A 119 (2015) 11623–11631.

[64] B. Finney, R.C. Fortenberry, J.S. Francisco, K.A. Peterson, A spectroscopic case for SPSi detection: The third-row in a single molecule, J. Chem. Phys. 145 (2016) 124311.

[65] J.M.L. Martin, P.R. Taylor, Accurate *ab Initio* quartic force field for *trans*-HNNH and treatment of resonance polyads, Spectrochim. Acta A 53 (1997) 1039–1050.

[66] B.R. Westbrook, R.C. Fortenberry, Anharmonic frequencies of $(MO)_2$ & related hydrides for M=Mg, Al, Si, P, S, Ca, & Ti and heuristics for predicting anharmonic corrections of inorganic oxides, J. Phys. Chem. A 124 (2020) 3191–3204.

[67] E.S. Doerksen, R.C. Fortenberry, A coincidence between bond strength, atomic abundance, and the composition of rocky materials, ACS Earth Space Chem. 4 (2020) 812–816.